Bulletin of the Seismological Society of America, Vol. 69, No. 1, pp. 135–158, February 1979

# ESTIMATING THE SEISMICITY FROM GEOLOGICAL STRUCTURE FOR SEISMIC-RISK STUDIES

BY JOHN G. ANDERSON

ABSTRACT

**Starting with geological data, this paper estimates the seismicity for applications in seismic risk studies. The rate at which seismic moment is released can be estimated on a fault when the slip rate is known. It can also be estimated in a region of crustal convergence (without subduction) or divergence when the rate at which opposite sides of the zone are converging or the regional strain rate is known. Then, provided all of the deformation is released seismically, by assuming the relative frequency of different sizes of earthquakes, the absolute frequency of events can be obtained.**

**The procedure is used to estimate seismicity in southern California. A review of geological literature has provided preliminary estimates of slip rates on many important faults. The estimates of the seismicity resulting from these slip rates are consistent with historical records of earthquake occurrences for southern California taken as a whole. For smaller regions or individual faults in southern California, the seismicity estimated from slip rates may differ from historical rates of seismicity by a factor of two or more. In the western basin and range region, the historical seismicity is also consistent with an estimate for the strain rate. Because of this agreement in larger regions, where many faults are involved, it is inferred that the geological data is also useful for studies of smaller regions, even though on this scale the model cannot be tested because of the too short historical record of earthquake occurrences.**

## INTRODUCTION

The outcome of a seismic risk analysis depends critically on the description of the seismicity used as input (Anderson and Trifunac, 1978). This paper addresses how to best describe the seismicity. "Seismicity" is used here to mean a complete description of the locations, sizes, and occurrence rates of earthquakes in a region. In a large enough region, the occurrence rate of earthquakes often seems well determined (e.g., Allen *et al.*, 1965). But the seismic risk at a specific site is most sensitive to the distribution of earthquakes near that site, for example, within 25 to 50 km. On this scale, the historical record is usually too short to estimate the seismicity. Geological studies on this scale are routine, however, and Allen (1975) has emphasized their usefulness for studies of the seismic hazard. This paper presents a framework for using these geological studies to obtain input to a seismic risk model.

Seismicity estimated from geological structure will be referred to here as the "geological seismicity." These estimates are for occurrence rates of earthquakes over a time interval of $10^3$ to $10^7$ years. This may be contrasted with the "historical seismicity," based on felt reports, which has a time scale of $10^2$ to $10^3$ years, and with "instrumental seismicity," which is known for a time scale of $10^1$ to $10^2$ years.

For the input to a risk analysis, a description of what Allen *et al.* (1965) refer to as the "secular seismicity" is most desirable. This could be derived from an instrumental or historical record which is much longer than the average recurrence interval of large earthquakes on all the faults near the site. But since these recurrence intervals may often be $10^2$ to $10^5$ years, a detailed description of the secular seismicity is practically impossible to obtain from the historical or the instrumental seismicity. Significant periodicities of occurrence or an earthquake prediction could, at times, demonstrate that the secular average is too high or too low for risk calculations for a coming short-time interval.

The geological record can often be interpreted to obtain fault slip rates or regional strain rates; these rates determine the geological seismicity. After presenting the necessary formulas, the paper focuses on southern California, where a preliminary estimate for the slip rates on most major faults is found from geological data. Several consistency checks are possible: the known slip rates on major faults are compared with slip rates derived from the rigid plate assumption in plate tectonic theory, these slip rates are used in three ways to estimate the geological seismicity, and the geological seismicity is compared with the historical seismicity. Agreement between the geological seismicity and the historical seismicity on the scale of southern California implies that both methods give a good estimate for secular seismicity there. Geological seismicity can also be estimated for the basin and range province on the basis of suggested strain rates; there, too, it is consistent with the historical seismicity. It is thus inferred that the geological seismicity may be used to estimate the secular seismicity in smaller regions when the historical record is too short.

## Relation Between Plate Movements and Seismic Moment

The seismic moment of an earthquake is proportional to the average slip on the fault during the earthquake, and the sum of the moments of all the earth quakes on a fault is proportional to the total seismic slip of the fault (e.g., Brune, 1968; Davies and Brune, 1971; Thatcher *et al.*, 1975). Therefore, if all the slip which accumulates because of plate tectonic motion is relieved in earthquakes, then the slip rate on the fault is directly related to the seismicity on that fault. These can be related through the seismic moment. Therefore, $\dot{M}_0$ is defined as the rate at which moment must be released from earthquakes on a fault or in a region to exactly relieve the annual slip across that fault or region. The product of $\dot{M}_0$ and a time interval gives a seismic moment which ideally equals the sum of the moments of all earthquakes which occurred in that time interval. Since some slip can occur aseismically (e.g., Kanamori, 1977b), $\dot{M}_0$ gives an upper limit to the seismicity.

For slip on a fault, from Brune (1968)

$$\dot{M}_0 = \mu A s \tag{1}$$

where $\mu$ is the shear modulus, $A$, is the area of the fault which is involved in seismic slip, and $s$ is the relative slip rate (per year) of opposite sides of the fault. Figure 1a shows the geometry of this situation. Equation (1) applies regardless of the width of the seismic zone, w in Figure 1a, provided all the faults are parallel to the plate margin. Davies and Brune (1971) have therefore applied equation (1) to plate margins worldwide, and found that seismicity is generally consistent with rates of plate motions.

Some earthquakes result from deformation of the plates in a general boundary region, particularly where the boundary is not regular or well defined. Seismicity in central Asia (Chen and Molnar, 1977) and in the transverse ranges of southern California may be examples of this mechanism. In these regions, if the slip rates on all the faults are known, equation (1) can still be applied. But a statistical procedure for going from the rate of convergence of two plates or microplates directly to $\dot{M}_0$ is also possible, using relations suggested by Kostrov (1974) and Chen and Molnar (1977). This is derived in Appendix I. The result is

$$\dot{M}_0 = |2\mu l_1 l_3 s/0.75|. \tag{2}$$

The product $l_1 l_3$ gives the cross-sectional area of the plates or microplates in a plane normal to the direction of convergence, and $s$ is the rate of convergence or divergence. Figure 1b shows the geometry for this case. The quantity 0.75 is an empirical constant, which conceivably could be regionally dependent. It was derived from central Asian data, and will be shown consistent with two micro plates in southern California.

If the region has width $l_2$,then the rate $s$ at which the opposite boundaries converge is related to the average strain rate within the convergent zone, $\dot{\epsilon}_{22}$, by $s = \dot{\epsilon}_{22} l_2$. Thus, equation (2) can be used with either convergence rates or strain rates.

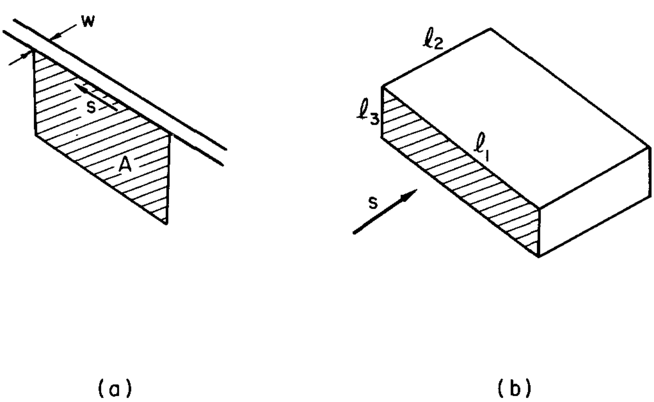


FIG. 1. Diagram of the types of relative plate motion considered to derive the seismicity. (a) Slip between two plates, occurring in a zone of width w. (b) Convergence or divergence resulting in seismic deformation.

## Relation Between Total Moment and Recurrence Curves

The parameter $\dot{M}_0$ defines the overall level of the seismicity, but gives no information about the frequency of earthquakes of any selected size. To obtain this, it is necessary to know how earthquakes are distributed in size. Assume that $N(\gamma)\, d\gamma$ gives the long-term average rate of occurrence of seismic events with moments between $\gamma - d\gamma/2$ and $\gamma + d\gamma/2$, where $\gamma = \log_{10} M_0$. The moment rate is then

$$\dot{M}_0 = \int_{-\infty}^{\infty} 10^{\gamma} N(\gamma)\, d\gamma. \tag{3}$$

If the form for $N(\gamma)$ were known, then equation (3) provides one constraint for the parameters which define $N(\gamma)$.

The moments of earthquakes are not routinely tabulated, and thus $N(\gamma)$ is not known directly. However, the distribution of magnitudes of earthquakes is usually described by

$$N(M) = 10^{a-bM}, \tag{4}$$

where $N(M)\,dM$ gives the number of events with magnitude between $M - dM/2$ and $M + dM/2$. The number of events with magnitude between $M_1$ and $M_2$, say, is

$$\int_{M_1}^{M_2} N(M)\,dM = \frac{10^a}{b\,ln_e 10}\,(10^{-bM_1} - 10^{-bM_2}). \tag{5}$$

For small earthquakes in southern California, Thatcher and Hanks (1973) found the average relation

$$\gamma = 16.0 + \tfrac{3}{2}M, \tag{6}$$

where the magnitude $M$ is interpreted as the local magnitude, $M_L$. Equation (6) is also consistent with the relationship between the moment of great earthquakes worldwide and the magnitude $M_w$ (Kanamori, 1977a). Therefore, equation (6) appears to be a reasonable average relationship for events of all sizes in California.

Combined with the frequency-magnitude relationship (4), one obtains

$$N(\gamma) = 10^{c-d\gamma} \tag{7}$$

where

$$b = \tfrac{3}{2}d \tag{8a}$$

and

$$a = c - 16d + \log_{10}(\tfrac{3}{2}). \tag{8b}$$

Preliminary findings by Chinnery and North (1975) indicate the historical earthquake occurrences are consistent with equation (7) to the largest events observed. The numerical constants in equations (6) and (8) may need to be reconsidered for regions other than California. Assuming $N(\gamma)$ is zero outside some range $\gamma_{\min} \leqq \gamma \leqq \gamma_{\max}$ and integrating equation (7) in equation (3) gives

$$\dot{M}_0 = \frac{10^c}{(1-d)\,ln_e 10}\,10^{(1-d)\gamma}\Big|_{\gamma_{\min}}^{\gamma_{\max}}$$

Smith (1976) and Campbell (1977, 1978) deliver similar relationships. If $\gamma_{\max} \gg \gamma_{\min}$

$$\dot{M}_0 = \begin{cases} \dfrac{10^c}{(1-d)\,ln_e 10}\,10^{(1-d)\gamma_{\max}} & (1-d)>0 \quad \text{(9a)} \\[2ex] \dfrac{10^c}{(1-d)\,ln_e 10}\,10^{(1-d)\gamma_{\min}} & (1-d)<0 \quad \text{(9b)} \end{cases}$$

Clearly, for the assumed distribution function, a finite value for $\dot{M}_0$ requires that $\gamma_{max}$ be finite when $(1 - d) > 0$. Similarly, when $(1 - d) < 0$, $\gamma_{min}$ must be finite.

For many areas of the world

$$b \approx 1, \text{ implying from equation (8a)}$$
$$d \approx \tfrac{2}{3}.$$

Therefore, equation (9a) holds in these regions. If $d = \frac{2}{3}$, about 55 per cent of the total moment is released during events with $\gamma_{max} - 1 < \log M_0 < \gamma_{max}$, and about 95 per cent of the total moment is released in events with $\gamma_{max} - 2 < \log M_0 < \gamma_{max}$.

Equation (9a) contains three unknowns: $c$, $d$, and $\gamma_{max}$. The quantity $\gamma_{max}$ is probably fixed from fault geometry. Its determination is discussed in the next section. The $b$ value of a region, related to $d$ by (8a) may change with time, either in a precursory period to a major earthquake, or in aftershock sequences (e.g., Scholz *et al.*, 1973; Bolt *et al.*, 1977). Even in a region where $b$ fluctuates, it may have a stable average over long time periods. If it is given the regional value observed from historical data, only $c$ remains to be estimated; it is found from equation (9a).

## Seismicity in the Southern California Region

For a trial application, the seismicity for the southern California region is estimated. Since both the geology and the seismicity of the region have been studied extensively, this is a good area to test the ideas in the preceeding sections.

### *Plate tectonics constraints*

The tectonic motions in southern California are, apparently, more complex than simple right lateral slip between the Pacific and the North American plates. Superimposed on the plate motion, there is left lateral shear along the Garlock and associated faults which accommodates the basin and range extension east of the Sierra Nevada mountains (Davis and Burchfiel, 1973; Lawrence, 1976).

The rigid plate motion of the Pacific plate relative to the North American plate is 5.5 cm/yr in California (Minster *et al.*, 1974). Atwater and Molnar (1973) indicate that the current rate has held for the past 4.5 m.y., that between 4.5 and 10 m.y. the relative rate was 4 cm/yr, and that between 10 and 21 m.y. the rate could have been 1.3 cm/yr. Between about 21 and 29 m.y. the Pacific plate first contacted North America as the Farallon plate broke up between the Mendocino and the Murray fracture zone.

The slip appears to be distributed over a broad region of the western United States (Atwater, 1970), and thus, it is not necessary that the total slip must be accounted for in southern California. Since aseismic deformation cannot be ruled out, it would not be necessary to account for the entire 5.5 cm/yr by faulting, even if the region spanned the entire zone of deformation (e.g., Walcott, 1978).

This plate tectonic motion can give an overall estimate of moment rate and thus of seismicity. For the region between the California-Mexico border (~32.6°N) and 36°N, $\dot{M}_0$ is $1.24 \times 10^{26}$ dyne-cm/yr. This is based on a slip rate $s$ = 5.5 cm/yr and a seismicity zone 500 km long; here and throughout the seismicity zone is assumed 15 km deep and with a shear modulus $\mu = 3 \times 10^{11}$ dyne/cm$^2$ (e.g., Thatcher *et al.*, 1975). Davies and Brune (1971) followed this approach for a larger region of western North America. They found that the historical seismicity implied a slip rate of 1.3

cm/yr, but they used 60 km for the depth of the seismicity zone. If they had used 15 km depth for this region, the slip rate derived from seismicity would have been 5.2 cm/yr, in good agreement with the Minster *et al.* (1974) model.

*Slip rates on faults*

The geological literature was reviewed to find estimates of slip rates for the important faults in the southern California region. To define the scope, faults designated on the Fault Map of California (Jennings, 1975) as having either historical movement or major Quaternary movement were studied. The results are summarized in Table 1. All the selected faults are listed in Table 1 except for some that are either unnamed on Jenning's map or splayed from a larger fault.

To estimate geological slip rate, the relative offset of a rock unit across a fault, and the time period in which that offset occurred must be found. The time period

TABLE 1

PRELIMINARY SLIP RATE ESTIMATES FOR MAJOR, CURRENTLY ACTIVE FAULTS IN SOUTHERN CALIFORNIA

| Fault Zone | Offset Feature | Age[1] | Offset | Slip Rate[2] (mm/year) | Nature[3] | Reference |
|---|---|---|---|---|---|---|
| San Andreas (Parkfield) | Triangulation & Geodimeter Stations | 25* yrs | | 32±3 | RL | Savage & Burford (1973) |
| (Carrizo Plains) | Stream Deposits | 3430* yrs | 127±5m | 37±3 | RL | Sieh (1977) |
| (Cholame Valley to San Juan Baustista) | Lower Pliocene | 5* my | 160-200 km | 32-40(40) | RL | Dickinson et.al. (1972) |
| Rinconada | Early Pliocene | 6my | 18km | 3 | RL | Hart (1976) |
| San Gregorio-Hosgri | Marine Terraces | 200,000* yrs | | 6.3-13 | RL | Weber & Lajoie (1977) |
| | 7 features. youngest: late Miocene-early Pliocene | 5*-13* my | 80-115km | 6-23 | RL | Graham & Dickinson (1978) |
| San Juan | | | | | RL | |
| Ozena | | | | | RL | |
| Sierra Nevada & Owens Valley | Strain Stations Geodetic | 40* yrs | dip-slip | 1±1 | N | Savage et.al. (1975) |
| | | | strike-slip | 4±1 | RL | Savage et.al. (1975) |
| | Shoreline cut in Bishop Tuff | 700,000* yrs | 0.3km | 0.4 | N | Christiansen (1966) |
| | McGee (Nebraskan) Glaciation | 2my | 1.2km | 0.6 | N | Christiansen (1966) |
| | Total structural relief | 2.3*-7.4* my | 3.0-6.0km | 0.4-2.7 | N | Christiansen (1966) |

[1] Ages denoted by * are used by reference. Others estimated from Heirtzler *et al.* (1968) time scale.

[2] Rates in parentheses are preferred by reference.

[3] RL, right lateral; LL, left lateral; T, thrust; N, normal.

[4] Age suggested by Carter (1971) as reasonable beginning for Garlock faulting, based on 64 to 74 km total offset (Smith, 1962; Michael, 1966) and Carter's estimated slip rate of 8 mm/yr.

[5] Age given by Davis and Burchfiel (1973) for beginning of extension in basin and range province in this region. Used here because of proposed relationship between basin and range spreading and Garlock fault (Davis and Burchfiel, 1973; Lawrence, 1976) and proposed relationship between Garlock fault and faults in Mojave Desert (Garfunkle, 1974).

[6] Similarity of total displacements south of the transverse ranges with those farther north (Crowell, 1975) suggest that rates should also be similar.

TABLE 1—*Continued*

| Fault Zone | Offset Feature | Age[1] | Offset | Slip Rate[2] (mm/year) | Nature[3] | Reference |
|---|---|---|---|---|---|---|
| Panamint Valley | Alluvial Fans | 10,000* - 20,000*yrs | 20m | 1-2 | RL | Smith (1977) |
| Death Valley | | 8[4]-17[5]my | 8km | 0.5-1 | RL | Davis & Burchfiel (1973); Wright & Troxel (1967) |
| Garlock | Late Wisconsin(?) alluvium | | | (8) | LL | Carter (1971) |
| | Early Tertiary Faults | 8[4]-17[5]my | 74km | 4-9 | LL | Michael (1966) |
| | Late Mesozoic Dikes | 8[4]-17[5]my | 64km | 4-8 | LL | Smith (1962) |
| Pinto Mountain | Pre-Cenozoic rocks & structure | 8[4]-17[5]my | 16km | 1-2 | LL | Dibblee (1975) |
| | | 8[4]-17[5]my | 5km | 0.3-0.6 | LL | Garfunkle (1973) |
| Big Pine | Post-Miocene | 7 | 6.4-16km | 1-2 | LL | Lamar et.al. (1973) |
| | Late Pliocene | 3* | 6.4 | (2) | LL | Lamar et.al. (1973) |
| Helendale | | 8[4]-17[5]my | 10-15km | 0.5-1.7 | RL | Garfunkle (1974) |
| Lockhart-Lenwood | | 8[4]-17[5]my | 15-20km | 0.9-2.5 | RL | Garfunkle (1974) |
| Harper | | | | | RL | |
| Camp Rock-Emerson | | 8[4]-17[5]my | 10km | 0.6-1.2 | RL | Garfunkle (1974) |
| Blackwater | | | | | RL | |
| Calico-West Calico | | 8[4]-17[5]my | 10-20km | 0.6-2.4 | RL | Garfunkle (1974) |
| Pisgah-Bullion | | 8[4]-17[5]my | 20-40km | 1.2-5.0 | RL | Garfunkle (1974) |
| Ludlow | | | | | RL | |
| Imperial Valley | Geodetic stations 0.33±0.05μ strain/yr over ~110km, including Elsinore, San Jacinto & San Andreas faults | 6* yrs | | 36±5 | | Prescott et.al. (1978) |

| Fault Zone | Offset Feature | Age[1] | Offset | Slip Rate[2] (mm/year) | Nature[3] | Reference |
|---|---|---|---|---|---|---|
| Imperial Valley | Geodetic Stations, spanning San Andreas & San Jacinto fault zones (0.4 strain/yr over 100km) | 26* yrs | | 40 | RL | Savage & Burford (1970) |
| San Andreas System (east of San Gabriel fault) | Lower Pliocene | 6* my | 240km | 40 | RL | Ehlert & Ehlig (1977) |
| | Upper Miocene & older | 4*-7* my | 240km | 34-60[6] | RL | Crowell (1975) |
| San Jacinto | Geodetic Stations (assuming depth of faulting = 15km) | 6 yrs | | 21±5 | RL | Savage & Prescott (1976) |
| | Stream - minimum age based on offset if slip rate is 25mm/yr, but is consistent with scarp appearance | 30,000*-50,000* yrs | 0.7km | 14-25 | RL | Sharp (1967) |
| | Quaternary Beds - minimum age based on offset if slip rate is 25mm/yr, but is consistent with stratigraphy | 0.2*-2* my | 5.1km | 2.5-25 | RL | Sharp (1967) |
| | Pliocene Beds | 2my | 18km | 9 | RL | quoted by Sharp (1967) |
| | Basement | | 25km | | | Sharp (1967) |
| Whittier-Elsinore | Lower Pliocene | 6* my | 4.8km | 0.8 | RL | Lamar et.al. (1973) |
| | Paleocene (offset post mid-Miocene) | 10-15my | 40km | 2.7-4 | RL | Sage (1973) |
| | Paleocene | 10-15my | 9-11km | 0.6-1 | RL | Weber (1977) |
| Chino | Late Miocene or early Pliocene | 6-10my | 0.4-0.7km | .04-.12 | T | Yerkes et.al. (1965) |

TABLE 1—*Continued*

| Fault Zone | Offset Feature | Age[1] | Offset | Slip Rate[2] (mm/year) | Nature[3] | Reference |
|---|---|---|---|---|---|---|
| Newport-Inglewood | Late Pliocene | 2my | 1.2km | 0.6 | RL | Wright et.al. (1973) |
| | Upper Miocene | 10my | 3km | 0.3 | RL | Yeates (1973) |
| Rose Canyon | Mid-Late Pliocene | 2-4my | 4km | 1-2 | RL | Kennedy (1975) |
| Palos Verdes | Mid-Late Pleistocene | 0.6my | 0.4km | 0.7 | T | Yerkes et.al. (1965) |
| San Clemente | Topography | | 40km | | RL | Shepard & Emery (1941) |
| San Gabriel | Upper Pliocene | | unfaulted | 0 | | Ehlig (1973) |
| | Upper Pliocene | 3*my | unfaulted | 0 | | Crowell (1973) |
| | Formations older than 13my | 13my | 60km | 5 | RL | Ehlig (1973) |
| Banning | | | | | | |
| Sierra Madre - Cucamonga | Alluvium | 10,000 - 30,000*yrs | 250m | 8-24(8) | T | Lamar et.al. (1973) |
| Malibu Coast | | | | | | |
| Santa Monica | Base of Lower Pliocene | 7my | 0.9km | 0.13 | T | Yerkes et.al. (1965) |
| | Base of Upper Miocene | 13my | 2.0km | 0.15 | T | Yerkes et.al. (1965) |
| Raymond | Post Miocene | 7my | 0.9-1.2km | 0.13-0.17 | T | Yerkes et.al. (1965) |
| Santa Cruz Island | | | | | | |
| Santa Susana | Plio-Pleistocene | 2my | 2.5km | 1.2 | T | Barnhart & Slosson (1973) |
| Oakridge | Upper Pliocene | 3-6my | 0.9-1.5km on figure | 0.2-0.5 | T | Quick (1973) |
| Arroyo Parida-San Cayetano | Upper Miocene - Lower Pliocene | 6my | 0.3km | 0.05 | T | Dibblee (1966) |
| Santa Ynez | Post Lower Miocene | | several mi. | | T | Dibblee (1966) |
| Pine Mountains | | | | | | |
| Pleito | | | | | T | |
| White Wolf | Miocene | 7my | 3km | 0.4 | T | Lamar et.al. (1973) |

depends on dating the offset features; thus, it has the largest errors. The ages of offset strata were often estimated from the Heirtzler *et al.* (1968) time scale. Age of the offset feature gives an upper limit to the time it took the offset to develop, but this does not necessarily cause the slip rate to be underestimated since the rate may be decelerating. Since plate motion has accelerated in the last 10 m.y. (Dickinson *et al.*, 1972; Atwater and Molnar, 1973), averages for time periods of this duration or longer may tend to underestimate the slip rate.

An important assumption is that the slip rate is the same along the entire length of the fault. The assumption cannot often be improved upon with the data in the geological literature. The Alpine fault in New Zealand may be a significant example of a fault with a nonuniform slip rate (Walcott, 1978).

Estimates for the slip rate and the derived seismicity are summarized in Table 2. Selection of slip rates for Table 2 from the ranges of data in Table 1 is occasionally arbitrary. Also on Table 2, the moment rate, $\dot{M}_0$, is given from equation (1). The fault length is measured from Jennings (1975).

A common practice in earthquake engineering is to estimate the maximum magnitude, $M_{\max}$ from the total length of the fault. It is assumed that the earthquake will rupture at most half of the fault length; this half-length is associated with a magnitude using a linear relationship between magnitude and log of rupture length (e.g., Slemmons, 1977, p. 115). The maximum magnitude in Table 2 is found using this procedure and the magnitude-rupture length relationship of Thatcher and Hanks (1973) for a stress drop of 100 bars. (Thatcher and Hanks contains a misprint; the correct relationship is $\log L = \frac{2}{3}M_L - 2.1 - \frac{2}{3}\log \Delta\sigma$, where $\Delta\sigma$ is the stress drop in bars.) For a selected rupture length, this implies a larger magnitude than many average formulas (e.g., See Slemmons, 1977). However, it provides a reasonable bound for much of the existing data gathered by Slemmons (1977) and Thatcher and Hanks (1973). A bound such as this is needed to find the upper bound magnitude. However, because Kanamori (1977a) finds $M_w = 8$ for the 1857 earthquake, larger magnitudes were not used on any faults. The suggestion by Allen (1968) that earthquakes larger than $M \cong 7\frac{1}{2}$ do not occur in the Imperial Valley further limits the estimate of $M_{\max}$ for the faults there.

The seismicity is sensitive to the estimate of $M_{\max}$. An increase of $M_{\max}$ of 0.5 will cause the number of events at any magnitude which is not affected by the change in cutoff to decrease by a factor of about 2. Furthermore, because of this decrease, the probability of exceeding a selected amplitude of shaking, when found by a seismic risk method such as Anderson and Trifunac (1978) or Cornell (1968) may actually decrease as $M_{\max}$ increases.

TABLE 2

ESTIMATES FOR SLIP RATE AND DERIVED SEISMICITY

| Region or Fault | Map Code | Fault Length (km) | Slip Rate (mm/year) | Nature of Motion* | $\dot{M}_0$ (dyne-cm/yr) | $M_{\max}$ |
|---|---|---|---|---|---|---|
| West of Sierra Nevada | | | | | | |
| San Andreas (San Luis Obispo to Cajon Pass) | SA | 475 | 37 | RL | $7.9 \times 10^{25}$ | 8 |
| Rinconada | RN | 200 | 3 | RL | $2.7 \times 10^{24}$ | 8 |
| San Gregorio - Hosgri | SGH | 380 | 10 | RL | $1.7 \times 10^{25}$ | 8 |
| San Juan | SJ | 65 | | RL | | 7½ |
| Ozena | OZ | 75 | | RL | | 7½ |
| East of Sierra Nevada Mts. | | | | | | |
| Sierra Nevada (Olancha to Garlock Fault) | SN | 115 | 0.5<br>4 | N<br>RL | $2.1 \times 10^{24}$ | 8 |
| Panamint Valley (Ballarat to Garlock) | PV | 65 | 1.5 | RL | $4.4 \times 10^{23}$ | 7½ |
| So. Death Valley (Jubilee Pass to Garlock Fault) | DV | 50 | 1 | RL | $2.3 \times 10^{23}$ | 7½ |
| Garlock & Related Faults | | | | | | |
| Garlock | GK | 255 | 8 | LL | $9.2 \times 10^{24}$ | 8 |
| Pinto Mountain | PM | 75 | 1 | LL | $3.4 \times 10^{23}$ | 7½ |
| Big Pine | BP | 70 | 2 | LL | $6.3 \times 10^{23}$ | 7½ |
| Mojave Desert | | | | | | |
| Helendale | HE | 90 | 1 | RL | $4.1 \times 10^{23}$ | 7½ |
| Lockhart-Lenwood | LL | 140 | 1.5 | RL | $9.5 \times 10^{23}$ | 8 |
| Harper | HA | 75 | | | | 7½ |
| Camp Rock-Emerson | CR | 75 | 1 | RL | $3.4 \times 10^{23}$ | 7½ |
| Blackwater | BW | 45 | | | | 7 |
| Calico-West Calico | CA | 95 | 1 | RL | $4.3 \times 10^{23}$ | 7½ |
| Pisgah-Bullion | PB | 100 | 2 | RL | $9.0 \times 10^{23}$ | 7½ |
| Ludlow | LU | 70 | | | | 7½ |

* RL, right lateral; LL, left lateral; T, thrust; N, normal.

† Approximate difference between total Imperial Valley slip and San Jacinto fault zone.

‡ Estimate with very large errors from qualitative data in Table 1.

TABLE 2—*Continued*

| Region or Fault | Map Code | Fault Length (km) | Slip Rate (mm/year) | Nature of Motion* | $\dot{M}_o$ (dyne-cm/yr) | $M_{max}$ |
|---|---|---|---|---|---|---|
| South of Transverse Ranges | | | | | | |
| San Andreas (Cajon Pass - Imperial Valley end) | SA | 200 | 15† | RL | $1.4 \times 10^{25}$ | 7½ |
| San Jacinto | SJC | 245 | 20 | RL | $2.2 \times 10^{25}$ | 7½ |
| Elsinore | EL | 235 | 1 | RL | $1.1 \times 10^{24}$ | 8 |
| Chino | CH | 25 | .07 | T | $7.9 \times 10^{21}$ | 7 |
| Newport-Inglewood | NI | 60 | 0.6 | RL | $1.6 \times 10^{23}$ | 7½ |
| Rose Canyon | RC | 55 | 1.5 | RL | $3.7 \times 10^{23}$ | 7½ |
| Palos Verdes | PS | 75 | 0.7 | T | $2.4 \times 10^{23}$ | 7½ |
| San Clemente | SC | 120 | | | | 8 |
| San Gabriel | SG | 100 | | | | 7½ |
| East Transverse Ranges | | | | | | |
| San Andreas-Mission Creek (Cajon Pass to Indian Hills) | NSA | 125 | 15† | RL | $8.4 \times 10^{24}$ | 7½ |
| Banning | BN | 75 | | | | 7½ |
| Central Transverse Ranges | | | | | | |
| San Andreas (Hwy 33/166 to Cajon Pass) | SA | 195 | 37 | RL | $3.2 \times 10^{25}$ | 8 |
| Sierra Madre - Cucamonga | SMC | 105 | 8 | T | $3.8 \times 10^{24}$ | 7½ |
| Malibu Coast - Raymond | MR | 90 | 0.15 | T | $6.1 \times 10^{22}$ | 7½ |
| Santa Cruz Island | | | | | | |
| Santa Susana | SS | 40 | 1.2 | T | $2.2 \times 10^{23}$ | 7 |
| Pleito | PL | 45 | | T | | 7 |
| White Wolf | WW | 55 | 0.4 | T | $9.9 \times 10^{22}$ | 7½ |
| West Transverse Ranges | | | | | | |
| Oakridge | OR | 45 | 0.3 | T | $6.1 \times 10^{22}$ | 7 |
| Santa Cruz Island | SCI | 60 | | | | 7½ |
| Arroyo Parida-San Cayetano | AP | 105 | 0.05 | T | $2.4 \times 10^{22}$ | 7½ |
| Pine Mountain | NM | 60 | | | | 7½ |
| Santa Ynez | SY | 135 | 2‡ | T | $1.2 \times 10^{24}$ | 8 |

Slip rates from Table 2 are shown on the map in Figure 2. This map is a Mercator projection about the pole of rotation given by Minster, *et al.* (1974), in the manner used by Atwater (1970). For rigid plate motion, the sum of all the horizontal (on this map) components of right lateral strike slip rates along any vertical line across this map should come to 5.5 cm/yr, the relative slip rate of the two plates. North of the transverse ranges, this sum is very close to the plate tectonic rate. South of the transverse ranges, the sum is only about 42 mm/yr; thus, not all the relative motion is accounted for.

The annual moment release in southern California may be obtained by summing the moments estimated for each of the faults in Table 2. To compare with the plate tectonics estimate in the last section, the following adjustments are needed: (1) sections of faults north of 36°N must not be counted (170 km of the San Andreas, 110 km of the Rinconada, 230 km of the San Gregorio-Hosgri, and 30 km of the Sierra Nevada fault zones must be deleted); (2) sections of the San Andreas fault

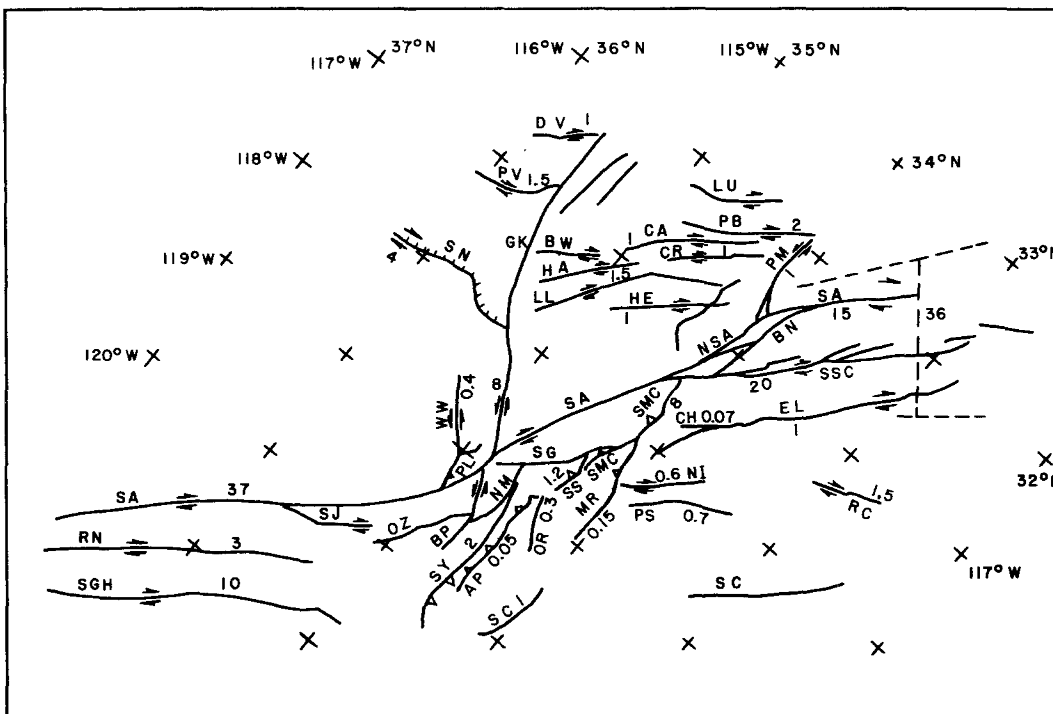


FIG. 2. Fault map of the southern California region on a Mercator projection about the pole of rotation of the Pacific plate relative to the North American plate, 50.9°N, 66.3°W (Minster *et al.*, 1974). Letter codes identify faults that are listed in Table 2. The teeth and ticks on some faults point in the direction of dip of thrust and normal faults, respectively. Slip rates, in mm/yr, are those given in Table 2. The light dashed lines at *right* show the approximate limits of the Salton geodetic net (Prescott *et al.*, 1978), and the slip rate across Imperial Valley estimated from that net. On this projection, the horizontal components of right lateral slip on any vertical cross section should sum to the relative rate of motion between the plates (55 mm/yr), provided all motion occurs by slip on faults between rigid blocks and the entire zone of deformation is spanned.

zone which are listed with both the transverse range faults and with those of adjoining sections must only be counted once. Making these adjustments, the moment rate from Table 2 becomes $1.16 \times 10^{26}$ dyne-cm/yr.

The rigid plate hypothesis in the previous section gave practically the same result: $1.24 \times 10^{26}$ dyne-cm/yr. The estimate from summing fault slip rates is not larger than the rigid plate method because of the missing motion south of the transverse ranges. The effect of adding that is small, however. Another fault the length of the San Jacinto fault with 15 mm/yr slip would bring the total to $1.33 \times 10^{26}$ dyne-cm/yr.

*Apparent shortage of slip south of the transverse ranges*

The right lateral slip rates summarized in Figure 2 total to about 40 mm/yr south of the transverse ranges, compared with about 55 mm/yr north of the transverse ranges and 55 mm/yr total plate motion (Minster *et al.*, 1974). Thus, about 15 mm/yr is not accounted for in southern California. If the geodetic data for the Imperial Valley are reasonably correct (they are consistent with the rate for the San Andreas fault where it bounds the transverse ranges immediately to the north), then the most likely possibility is that strike slip motion takes place offshore from southern California. From the geometry of Figure 2, it appears difficult for the motion which occurs west of the San Andreas fault on the north side of the transverse ranges to occur east of the San Andreas fault south of the transverse ranges. The slip in the transverse ranges seems to be thrusting and left lateral motion, contradicting the hypothesis that a large amount of right lateral slip changes sides of the San Andreas there. The possibility that the missing relative motion does not occur on any major fault, as in part of New Zealand (Walcott, 1978) cannot be ruled out, but the geodetic data at least would include ductile deformation in the Imperial Valley.

Little is known about the offshore faults mapped by Jennings (1975), but both the Palos Verdes (Yerkes *et al.*, 1965) and the San Clemente (Jennings, 1975) faults show evidence of major Quaternary movement. The large earthquake which occurred in 1892 in Baja, California (Richter, 1958, pp. 531 to 533) may support this hypothesis. It could have occurred on either the Agua Blanca fault or the San Miguel fault; both have components of right-lateral strike-slip (Richter, 1958). The trends of the Agua Blanca fault and San Clemente fault suggest that they could be connected (e.g., Johnson *et al.*, 1976). If the 1892 earthquake ruptured the width of Baja, California on a strike parallel to the Agua Blanca fault (~200 km) to a depth of 15 km, the moment of $5 \times 10^{26}$ dyne-cm suggested by Hanks *et al.* (1975) implies an average dislocation of 5.5 meters. If such an event occurs once every 500 yr, consistent with the rate of occurrence of smaller events in the region reported by Hileman *et al.* (1973), the slip rate along the fault would be 11 mm/yr. This is about the amount of slip which is not accounted for farther north. This argument is entirely speculative; furthermore, the relationship between the Agua Blanca and San Miguel faults and faults in the Gulf of California is not known (Johnson *et al.*, 1976). But the result suggests that about 20 per cent of the relative plate motion in southern California between the transverse ranges and the Mexican border may occur on offshore faults.

*Rates of convergence: A consistency check*

In principle, the slip rates can be used to estimate the rates of convergence of small crustal blocks in the transverse ranges, where the convergence is caused by the bend in the San Andreas fault. These convergence rates can then be used with equation (2) to find $\dot{M}_0$. This can be compared with the value of $\dot{M}_0$ derived from the slip rates on faults in the convergent area. This checks, in another region, the empirical constant of 0.75 used in equation (2).

From the slip rates in Table 1, illustrated on Figure 2, the block between the San Andreas and San Jacinto faults is converging on the Mojave Desert at about 15 mm/yr. The region between the San Jacinto and the Newport-Inglewood fault (taken as the line which marks the southern extension of the San Andreas from Carrizo Plain) is converging on the Mojave Desert at about 35 mm/yr. The region west of Newport-Inglewood Fault zone is converging on the transverse ranges at between zero and 10 mm/yr, depending on where the motion actually occurs. There are not enough data to support a reasonable estimate of the convergence rate in this region.

Taking the width of the eastern block as 45 km, equation (2) predicts a total moment rate for this region of $8.1 \times 10^{24}$ dyne-cm/yr. We may compare this with the moments estimated for the major faults. Most important is the San Andreas; for the portion that bounds the north edge of this block, equation (1) predicts $\dot{M}_0 = 8.4 \times 10^{24}$ dyne-cm/yr. The result is sensitive to the selection of end points of the San Andreas fault; here they were taken at the junction of the Banning and Mission Creek branches in the southeast and the San Jacinto junction in the northwest.

Taking the central block to be 80 km wide, equation (2) predicts $\dot{M}_0 = 3.4 \times 10^{25}$ dyne-cm/yr for the region, while equation (1) predicts $3.2 \times 10^{25}$ dyne-cm/yr for the San Andreas fault alone. Other faults bring the total annual moment to $3.6 \times 10^{25}$ dyne-cm/yr.

The result suggests that the empirical constant 0.75 in equation (2) is reasonable for these two regions in southern California. However, equation (2) provides little information about secondary faulting where a master fault dominates the tectonics. The faulting and deformation in the transverse ranges seem to be such a second-order effect. The slip rate on the Sierra Madre fault, which appears to be second in importance to the San Andreas fault, implies that it releases only about 10 per cent of the total moment in the central region. Kosloff (1977) similarly concluded that if the transverse ranges are caused by the bend, the stress released by thrust faulting is small compared to the stresses released on the San Andreas fault.

*Comparison with historical seismicity*

For southern California as a whole, the recurrence interval of the larger events is comparable to the length of the historic record. Therefore, if the proposed method is reasonable, the geological seismicity may be consistent with historical seismicity. In smaller regions, the recurrence interval of large events begins to exceed the duration of the historical record; when this occurs, the geological seismicity may show no relationship to the historical seismicity.

*Southern California between Mexico and 36°N.* Hanks *et al.* (1975) estimated the moments of large events in southern California. For earthquakes with $M_0 \geqq 10^{27}$ dyne-cm, Hanks *et al.* (1975) list three events and estimated moments in this region: 1857, $9 \times 10^{27}$ dyne-cm; 1927, $1 \times 10^{27}$ dyne-cm; 1952, $2 \times 10^{27}$ dyne-cm. Hanks *et al.* (1975) believe this record is complete from 1857 through 1973, or for 117 years, giving $10.3 \times 10^{25}$ dyne-cm/yr from events of this size.

For events with $10^{25} \leqq M_0 < 10^{27}$, the record is complete from 1903 through 1973, or for 71 years. From their Table I, there are 14 such events, with a total of $112 \times 10^{25}$ dyne-cm, or $1.6 \times 10^{25}$ dyne-cm/yr from events in this size range. Since this is about one-tenth the contribution from events with $M_0 \geqq 10^{27}$, one can assume that events with $M_0 < 10^{25}$ contribute about one-tenth the annual rate of events with $10^{25} \leqq M_0 < 10^{27}$. Then, the historical rate at which moment is released is estimated from the sum over these three ranges of moments, and comes to $1.2 \times 10^{26}$ dyne-cm/yr. This compares very well with rates of about 1.16 to $1.24 \times 10^{26}$, obtained from the geological procedures. The close agreement may be somewhat fortuitous, as a different assumption about the depth of faulting or an improved model for slip rates could lead to different results.

*San Jacinto fault.* Thatcher *et al.* (1975) have used seismic moments of the largest earthquake on the San Jacinto fault to estimate a slip rate of 8 mm/yr. The largest contribution to the cumulative moment between 1890 and 1973 is from nine events, tabulated by Hanks *et al.* (1975), with $6.0 \leqq M_L \leqq 7.0$. The sum of the moments for these events is $6.9 \times 10^{26}$ dyne-cm (from Table 1, Thatcher *et al.*, 1975). This neglects small events. Equation (9a) indicates that if $b = 0.86$, and if $M_{\max} = 7.0$, then 23 per cent of the total moment should be expected from events with $M_L$ less than 6.0. Assuming this was so between 1890 and 1973, the moment from all events would have been $9.0 \times 10^{26}$ dyne-cm, or $1.1 \times 10^{25}$ dyne-cm/yr. This is about half the estimate of $2.2 \times 10^{25}$ dyne-cm/yr from Table 2. It is not known whether the discrepancy arises from too short a historical seismicity record, from a poor estimate of slip rate or depth of faulting, or from aseismic slip.

*Western transverse ranges.* We consider the region bounded by the latitudes 33°N and 35.5°N, and by the longitudes 117.5°W and 121°W. The eastern boundary was selected to exclude the higher activity along the San Jacinto fault. Earthquakes in the Los Angeles basin and offshore south of the transverse ranges are included.

TABLE 3

EVENTS IN REGION 33.0 TO 33.5°N, 117.5 TO 121°W, $M_L > 6$, FROM HANKS *ET AL.* (1975)

| Year | Description | Lat. | Long. | $M_L$ | $M_0$ ($\times 10^{25}$ dyne-cm) |
|---|---|---|---|---|---|
| 1857 | Ft. Tejon | | | 8.0* | 900 |
| 1916 | Tejon Pass | 34.9 | 118.9 | 6 | .1 |
| 1925 | Santa Barbara Channel | 34.3 | 119.8 | 6.3 | 20 |
| 1927 | Pt. Arguello | 34.5 | 121 | 7.5 | 100 |
| 1933 | Long Beach | 33.6 | 118.0 | 6.3 | 2 |
| 1941 | Santa Barbara Channel | 34.4 | 119.6 | 6.0 | 0.9 |
| 1952 | Kern County | 35.0 | 119.0 | 7.7 | 200 |
| 1952 | Aftershock | 35.0 | 119.0 | 6.4 | 3 |
| 1952 | Aftershock | 35.4 | 118.6 | 6.1 | 0.4 |
| 1952 | Aftershock | 35.4 | 118.9 | 6.1 | 3 |
| 1971 | San Fernando | 34.4 | 118.4 | 6.4 | 10 |
| 1973 | Pt. Mugu | 34.1 | 119.0 | 6.0 | 0.1 |

* Obtained from $M_0$ using $\log M_0 = 16.0 + \frac{3}{2}M$.

Table 3 lists the events inside this region which were studied by Hanks *et al.* (1975). They consider their data complete for events with $M_0 \geqq 10^{27}$ (or $M \gtrsim 7\frac{1}{2}$) from 1857 through 1973, and for events with $M_0 \geqq 10^{25}$ ($M \gtrsim 6$) from 1903 through 1973. Magnitudes are from Hanks *et al.* (1975) except for the 1857 earthquake, where the magnitude is estimated from the moment given by Hanks *et al.* (1975) using equation (6).

Table 4 summarizes the recurrence rates of earthquakes with magnitudes greater than 2.5 for the study region. The numbers of events with $M_L \leqq 6.0$ are from the Earthquake Data File maintained by the National Geophysical and Solar Terrestrial Data Center (Meyers and vonHake, 1976). Statistics of events with $M_L \geqq 6.5$ are from Table 3. No statistical test was made for completeness; Stepp (1972) states that the catalog is homogeneous in magnitude 4.0 and larger events since 1933 and in magnitude 3.0 and larger events since 1953. Historical seismicity rates are plotted in Figure 3.

## TABLE 4

OCCURRENCE RATES[1] OF EARTHQUAKES IN THE REGION 33.0 TO 35.5°N, 117.5 TO 121°W

| Center Magnitude | 2.5 | 3.0 | 3.5 | 4.0 | 4.5 | 5.0 | 5.5 | 6.0 | 6.5 | 7.0 | 7.5 | 8.0 |
|---|---|---|---|---|---|---|---|---|---|---|---|---|
| Observed Earthquakes[2] | 1952 to 1974 | | | | 1933 to 1974 | | | 1903 to 1977 | | | 1857 to 1977 | |
| Entire Region | 1147 | 1398 | 583 | 187 | 198 | 49 | 15 | 9 | 4 | 0 | 2 | 1 |
| San Andreas | | | | | | | | | | | | 1 |
| San Gregorio-Hosgri | | | | | | | | | | | 1 | |
| Long Beach (33.0-34.0°N,117.8-118.5°W) | 237 | 118 | 41 | 14 | 43 | 16 | 4 | 0 | 1 | | | |
| Kern County (34.8-35.5°N,118.4-119.1°W) | 259 | 673 | 185 | 50 | 97 | 23 | 7 | 5 | 1 | 0 | 1 | |
| San Fernando (34.2-34.7°N,118.2-118.65°W) | 184 | 186 | 152 | 67 | 18 | 3 | 1 | 2 | 1 | | | |
| Remainder | 467 | 321 | 205 | 56 | 35 | 7 | 3 | 2 | 1 | | | |
| Events/year (data) | | | | | | | | | | | | |
| Entire Region | 54 | 66 | 27 | 8.8 | 4.8 | 1.2 | .36 | .22 | .056 | - | .017 | .0085 |
| San Andreas | - | - | - | - | - | - | - | - | - | - | - | .0085 |
| San Gregorio-Hosgri | - | - | - | - | - | - | - | - | - | - | .0085 | |
| Long Beach (Newport-Inglewood) | 11 | 5.6 | 1.9 | .66 | 1.0 | .39 | .097 | - | .014 | - | - | |
| Kern County (White Wolf) | 14 | 32 | 8.7 | 2.4 | 2.3 | .56 | .17 | .12 | .014 | - | .0085 | |
| Events/year (Continued) | | | | | | | | | | | | |
| San Fernando (Sierra Madre) | 8.7 | 8.8 | 7.2 | 3.2 | .44 | .073 | .024 | .048 | .014 | - | - | |
| Remainder | 22 | 16 | 9.6 | 2.6 | .85 | .17 | .073 | .048 | .014 | - | - | |
| Events/year (Model) | | | | | | | | | | | | |
| Entire Region | | 106 | 39 | 14.6 | 5.5 | 2.1 | 0.75 | .28 | .10 | .038 | .013 | .0027 |
| San Andreas (280 km) | | 71.7 | 26.5 | 9.8 | 3.7 | 1.4 | .50 | .19 | .070 | .026 | .0096 | .0022 |
| San Gregorio-Hosgri (80km) | | 5.5 | 2.0 | 0.76 | .28 | .10 | .039 | .014 | .0053 | .0020 | .00074 | .00017 |
| Elsinore (185km) | | 1.3 | 0.49 | 0.18 | 0.068 | 0.025 | .0094 | .0035 | .0013 | .00048 | .00018 | .000042 |
| Chino | | .053 | .020 | .0073 | .0027 | .0010 | .00037 | .00014 | .000051 | .000013 | | |
| Newport-Inglewood | | 0.51 | 0.19 | 0.071 | .026 | .0098 | .0036 | .0013 | .00050 | .00019 | .000043 | - |
| Palos Verdes | | 0.77 | 0.29 | 0.11 | .039 | .015 | .0054 | .0020 | .00075 | .00028 | .000064 | |
| Garlock (150 km) | | 8.3 | 3.1 | 1.1 | .42 | .16 | .059 | .022 | .0081 | .0030 | .0011 | .00026 |
| Big Pine | | 2.0 | 0.75 | 0.28 | .10 | .038 | .014 | .0053 | .0020 | .00073 | .00017 | - |
| Sierra Madre | | 12 | 4.5 | 1.7 | .62 | .23 | .086 | .032 | .012 | .0044 | .0010 | - |
| Santa Susana | | 1.5 | .55 | .20 | .075 | .028 | .010 | .0039 | .0014 | .00032 | | |
| Oakridge | | .41 | .15 | .056 | .021 | .0078 | .0029 | .0011 | .00040 | .000091 | | |
| Malibu Coast-Raymond | | .20 | .072 | .027 | .010 | .0037 | .0014 | .00051 | .00019 | .000071 | .000016 | |
| Arroyo Parida | | .077 | .029 | .011 | .0039 | .0015 | .00054 | .00020 | .000075 | .000028 | .000006 | |

[1] Numbers of events with magnitude within 0.25 of center magnitude.

[2] Dates at head of column indicate time interval of observations. Data from NOAA earthquake data file and from Table 3.

TABLE 4—*Continued*

| Center Magnitude | 2.5 | 3.0 | 3.5 | 4.0 | 4.5 | 5.0 | 5.5 | 6.0 | 6.5 | 7.0 | 7.5 | 8.0 |
|---|---|---|---|---|---|---|---|---|---|---|---|---|
| Model (Continued) | | | | | | | | | | | | |
| Santa Ynez | | 1.8 | .68 | .25 | .094 | .035 | .013 | .0048 | .0018 | .00067 | .00025 | .000058 |
| White Wolf | | .32 | .12 | .044 | .016 | .0060 | .0022 | .00083 | .00031 | .00011 | .000027 | - |

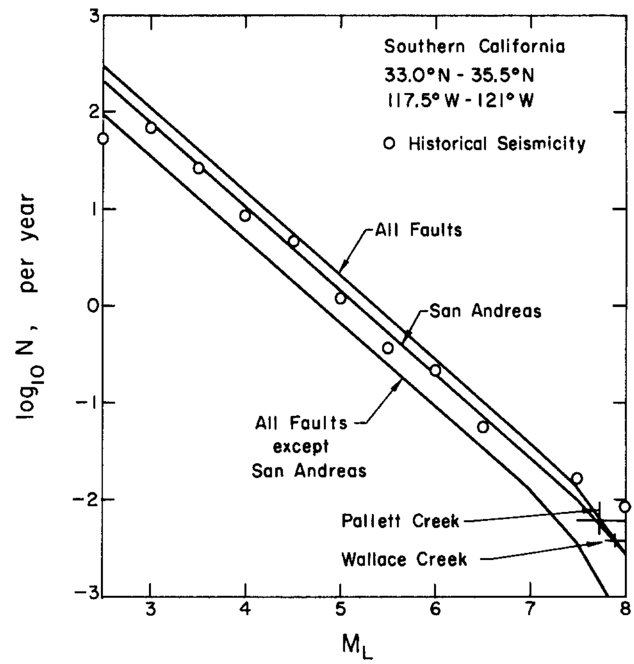


FIG. 3. Observed and predicted occurrence rates of earthquakes for the sub-region bounded by 33.0°N and 35.5°N, and 117.5°W and 121°W. Predicted rates are obtained by integrating equation (5) over intervals of $\frac{1}{2}$ magnitude width. The steeper slopes at larger magnitudes result when faults stop contributing to the total beyond their cut-off magnitude.

Table 4 also lists the numbers of earthquakes which have occurred in five smaller portions of the region. The main shock and aftershocks of the Long Beach (1933), Kern County (1952), and San Fernando (1971) sequences represent most of the activity on the Newport-Inglewood, White Wolf, and Sierra Madre faults during this time period. The 1857 earthquake is associated with the San Andreas fault; the 1927 earthquake is probably associated with the Hosgri fault, although this association is equivocal.

Table 4 also lists the occurrence rate at each magnitude predicted by the model for each of the faults which are either entirely or partially included. This uses $b$ = 0.86, after Allen *et al.* (1965), and the values of $\dot{M}_0$ and $M_{\max}$ from Table 2 to get $c$ from equation (9a). A log $N$ versus $M$ curve based on this sum is also plotted in Figure 3. The model overestimates the number of events per year with $M \leqq 7$, and underestimates the historical rate of events with $M \geqq 7\frac{1}{2}$. Differences are less than a factor of 2, except for $M_L$ = 8. The magnitude $7\frac{1}{2}$ and 8 data are based on so few earthquakes that the points cannot be considered reliable. Sieh (1977) provides data for recurrence rates of major events at two sites on the San Andreas fault: Pallett Creek and Wallace Creek. Rates implied from his data are also plotted on Figure 3.

It appears from Figure 3 that the geological seismicity is similar to the historical seismicity of this region. However, Table 4 shows that the observed occurrence rates for individual faults are nearly unrelated to the geological predictions; Allen *et al.* (1965) found a similar result. The San Andreas is a prominent example: although the slip rate implies that it should be the most active fault, it has been almost completely inactive since 1933. The high seismicity in the total is obtained because the Newport-Inglewood and the White Wolf faults have been considerably more active than one would predict from the geological data. The discrepancies may arise because the historic interval is so much shorter than the recurrence interval for the faults in the area.

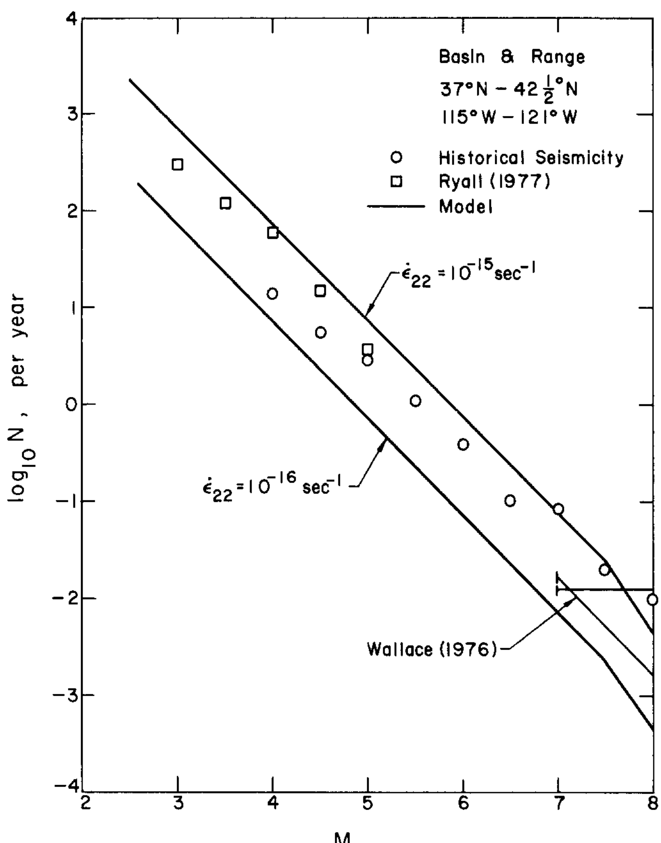


FIG. 4. Observed and model seismicity for the western basin and range region bounded by 37°N to 42.5°N and 115°W to 121°W. The historical seismicity is from Table 5. Data from Ryall (1977) are for years 1970 to 1974. Model uses maximum magnitude of 8.0 and b-value of 1.0, and is shown for extreme estimates of strain rate in the basin and range region from Lawrence (1976).

## Basin and Range Seismicity

Lawrence (1976) suggests that the strain rate in the basin and range province is between $10^{-15}$ sec$^{-1}$ and $10^{-16}$ sec$^{-1}$. With equation (2), this can be used to estimate the moment rate, and thus the seismicity in the basin and range province. We consider the same region as was considered by Ryall (1977), bounded by 37°N and 42.5°N latitudes and 115°W and 121°W longitudes. This gives an area of approximately $3.1 \times 10^5$ km$^2$. With equation (2), this implies $\dot{M}_0 = 1.2 \times 10^{25}$ to $1.2 \times 10^{26}$

dyne-cm/yr for this region. The implied recurrence curves for $M_{\max} = 8$ and for $b = 1.0$ are plotted in Figure 4. The estimate by Wallace (1976) that there is $4 \times 10^{-5}$ earthquakes/yr per $10^3$ km$^2$ with $M$ between 7 and 8 implies 0.012 events per year for this region. The horizontal line on Figure 5 shows this average rate from Wallace; the sloping line shows how these events would be distributed with a $b$-value of 1.0.

Since 1872, Ryall gives three earthquakes with magnitude greater than $7\frac{1}{4}$: 1872, Owens Valley ($M_w = 7.8$ based on moment estimate of Hanks *et al.*, 1975); 1915, Pleasant Valley, $M = 7.6$; 1932, Cedar Mountains, $M = 7.3$. Occurrence rates for smaller magnitudes are summarized in Table 5, with the data from the Earthquake Data File (Meyers and von Hake, 1976). These rates are plotted on Figure 5.

Finally, Figure 5 shows the seismicity rates for small earthquakes from 1970 to 1975, taken from Ryall (1977). For magnitudes about 4 to $4\frac{1}{2}$, the seismicity rates from Ryall (1977) are somewhat larger than from the Earthquake Date File tape, perhaps because Ryall used data from a local network with more complete coverage.

TABLE 5

OCCURRENCE RATES FOR EARTHQUAKES IN THE NEVADA REGION OF THE BASIN AND RANGE PROVINCE: 37°N TO $42\frac{1}{2}$°N, 115°W TO 121°W, BASED ON EARTHQUAKE DATA FILE (MEYERS AND VONHAKE, 1976) AND LARGE EARTHQUAKES TABULATED BY RYALL (1977)

| M | Time Interval, yrs | No. of Events | Rate, per year |
|---|---|---|---|
| 8 | 103.3 | 1 | .0097 |
| 7½ | 103.3 | 2 | .0194 |
| 7 | 48.3 | 4 | .0828 |
| 6½ | 48.3 | 5 | .103 |
| 6 | 42.3 | 17 | .402 |
| 5½ | 42.3 | 46 | 1.09 |
| 5 | 42.3 | 121 | 2.86 |
| 4½ | 42.3 | 240 | 5.67 |
| 4 | 42.3 | 584 | 13.8 |

It appears that the historical rates are slightly larger than the rates estimated from Wallace (1976), and the geological seismicity estimated from equation (2) is consistent with both the historical rates and Wallace's rates for a strain rate near the more rapid end of the range suggested by Lawrence (1976).

## CONCLUSION

Formulas drawn from the geophysical literature may be used in conjunction with geological data to estimate the seismicity of a region. In southern California, and in the western basin and range province, the method works well for the region as a whole. This implies that the method should also work well for smaller regions; in southern California, it does not agree as closely with the historic seismicity for subregions or individual faults, probably because in these regions the recurrence interval is longer than the historic record of earthquakes. Nonetheless, this agreement for the larger regions implies that where the historical record of earthquakes is brief, the procedures used here can significantly decrease the uncertainty of seismicity estimates.

To obtain the seismicity of southern California, a review of the geological literature gave preliminary estimates for the slip rates on various faults. North of the transverse ranges, most of the slip which is implied by tectonic studies can be accounted for on known faults. South of these ranges, however, over 10 mm/yr cannot yet be accounted for. A possible location for it is offshore in the Pacific Ocean; if so, about 20 per cent of the total seismic moment released in southern California is released offshore in a region where the risk to population is perhaps minimal. However, many of the slip rates used here are rather speculative. Refinements of the model are needed to obtain more reliable estimates of the seismic risk.

Methods suggested here could eventually help to understand the seismicity within lithospheric plates as well as at their margins. For example, if new geodetic methods (e.g., Bender and Silverberg, 1975; Coates *et al.*, 1975) detected deformation rates within plates over the next several years, relations suggested here could give seismicity estimates in these regions, as was done here for the basin and range region. This procedure could be helpful in understanding the activity in the eastern United States, for example.

## ACKNOWLEDGMENT

T. L. Henyey, T. L. Teng, and M. D. Trifunac critically reviewed the manuscript. This research was supported by the United States Nuclear Regulatory Commission, and by the U.S. Geological Survey, Department of the Interior, under USGS Grant 14-08-0001-G-501.

## APPENDIX I

Kostrov (1974) shows that for one earthquake, the elements of the moment tensor are

$$M_{ij} = M_0(b_i n_j + b_j n_i) \tag{A1}$$

where **n** is a unit vector normal to the fault and **b** is a unit vector in the direction of slip, assumed to be perpendicular to **n**. The principle axes of the moment tensor are $\mathbf{p}^{(1)} = (\mathbf{b} + \mathbf{n})\sqrt{2}$ and $\mathbf{p}^{(2)} = (\mathbf{b} - \mathbf{n})\sqrt{2}$, and the largest principle value is the scalar value of the moment, $M_0$ (Kostrov, 1974). The relationship of **b**, **n**, $\mathbf{p}^{(1)}$, and $\mathbf{p}^{(2)}$ is shown for a fault in a compressive environment in Figure I.1a. Kostrov shows that the strain rate $\dot{\epsilon}_{ij}$ in a region with volume $v$ is related to the moment tensor by

$$\dot{\epsilon}_{ij} = \frac{1}{2\mu} \frac{\sum_{k=1}^{K} M_{ij}^{(k)}}{v \Delta t} \tag{A2}$$

where the sum is over all seismic events, and $t$ is the time interval during which these events were recorded. We equate

$$\Sigma M_{ij}^{(k)}/\Delta t = M_{ij}^T/\Delta t = \dot{M}_{ij}.$$

Let the cartesian coordinate axes be oriented such that $x_3$ is vertical and $x_2$ is parallel to the direction of relative plate motion, and suppose the region which is being deformed between the plates can be approximated as a block with dimensions $l_1$, $l_2$, and $l_3$ parallel to these axes. The rate of plate motion $s$ is related to $\dot{\epsilon}_{22}$, the

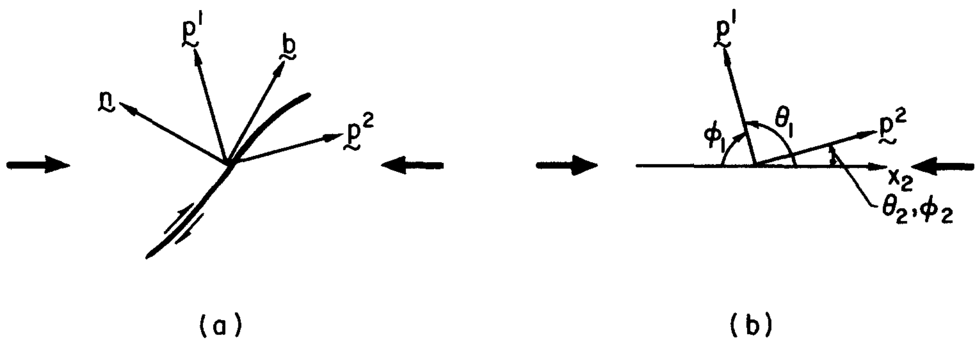


FIG. I.1. (a) Relationship of **b**, **n**, $\mathbf{p}^1$ and $\mathbf{p}^2$ for earthquake on a fault (heavy line) with sense of slip as indicated. Heavy arrows suggest a compressive environment for this fault, and thus define the direction of the $x_2$ axis. (b) Definition of $\theta_1$, $\theta_2$, $\phi_1$, $\phi_2$ assuming (a) conforms with the special case where $\mathbf{p}^1$, $\mathbf{p}^2$, and $\hat{x}_2$ are coplanar.

strain rate parallel to the plate motion, by $s = \dot{\epsilon}_{22} l_2$, and equation (A2) becomes

$$s = \frac{1}{2\mu} \frac{\dot{M}_{22}}{\left(\dfrac{v}{l_2}\right)}, \tag{A3}$$

or

$$\dot{M}_{22} = 2\mu l_1 l_3 s. \tag{A4}$$

The critical question now is how $\dot{M}_{22}$ is related to $\dot{M}_0$. For each event, $M_{22}^{(k)} = M_0^{(k)}(2b_2n_2)$. For shortening in the $x_2$ direction (plate convergence), $b_2n_2 < 0$, $\dot{\epsilon}_{22} < 0$, $s < 0$, and $M_{22}^T < 0$. It is easy to verify that

$$2b_2n_2 = (\mathbf{p}^{(1)} \cdot \hat{x}_2)^2 - (\mathbf{p}^{(2)} \cdot \hat{x}_2)^2. \tag{A5}$$

Let us define $\mathbf{p}^{(1)} \cdot \hat{x}_2 = \cos\theta_i$, where $\theta_i$ is the polar angle between the positive $x_2$ axis and the principle axis represented by $p^{(i)}$.

Since $\cos^2(180° - \theta) = \cos^2\theta$, we let $\phi_i$ be the acute angle between the $x_2$ axis and $p_i$. Then

$$\phi_i = \begin{cases} \theta_i & 0 \le \theta_i \le 90° \\ 180° - \theta_i & 90° < \theta_i \le 180° \end{cases}$$

and by equation (A5)

$$\begin{aligned} 2b_2n_2 &< 0 \qquad \phi_1 > \phi_2 \\ &> 0 \qquad \phi_1 < \phi_2. \end{aligned} \tag{A6}$$

Since the case where $2b_2n_2 < 0$ represents plate convergence and $2b_2n_2 > 0$ represents plate divergence, equation (A6) says that in a compressive environment, $\mathbf{p}^{(2)}$ more nearly parallels the direction of plate motion, and in an extensional environment, $\mathbf{p}^{(1)}$ more nearly parallels the direction of plate motion.

An important special case occurs when $\mathbf{p}^{(1)}$, $\mathbf{p}^{(2)}$, and $\hat{x}_2$ are coplanar. This includes vertical strike-slip faults and faults that strike perpendicular to the $x_2$ axis and have entirely dip-slip motion. In this situation, shown in Figure I.1b, $\phi_1 + \phi_2 = 90°$. Thus, from equation (A5)

$$2b_2n_2 = \cos 2\phi_1 = -\cos 2\phi_2. \tag{A7}$$

In a compressional environment, we expect $\phi_2 < 45°$, so that by equation (A7) $2b_2n_2 < 0$. It is not necessary to assume that $\phi_2 = 0$ for all events; one might instead expect some probability distribution for $\phi_2$ or $\theta_2$. As an example, suppose that in an ensemble of events, $\theta_2$ occurs randomly in a uniform distribution between 0 and 45°. Then

$$p(\theta_2) = \begin{cases} \dfrac{4}{\pi} & 0 \le \theta_2 \le \dfrac{\pi}{4} \\ 0 & \text{otherwise} \end{cases} \tag{A8}$$

and

$$\frac{\overline{M}_{22}}{-M_0} = \int_0^{\pi/4} p(\theta_2) \cos 2\theta_2 \, d\theta_2 = \frac{2}{\pi} \approx 0.64$$

or

$$\overline{M}_{22} \cong -0.64 M_0. \tag{A9}$$

In reality, one may expect $\theta_2$ to be concentrated more toward zero, and thus expect the empirical constant to be somewhat larger than 0.64.

It is difficult to relax the assumption that $\mathbf{p}^{(1)}$, $\mathbf{p}^{(2)}$, and $\hat{x}_2$ are coplanar since assumptions about the joint probability distributions of $\phi_1$ and $\phi_2$ are needed. It would be preferable to obtain an empirical estimate to replace equation (A9). This is possible by using the data from Chen and Molnar (1977).

In Table I of Chen and Molnar, $M_0{}^T = 1.2 \times 10^{29}$ for major events in central Asia from 1911 to 1967. They find, in their equations (5a), that along the principle axes of extension and compression for that time period that, in our notation, $M_{11}^T = 9.4 \times 10^{28}$ and $M_{22}^T = -8.8 \times 10^{28}$. Thus, one obtains

$$M_{11}^T = 0.78\, M_0{}^T$$

and

$$M_{22}^T = -0.73\, M_0{}^T.$$

This empirical estimate of the relationship of the elements of the moment matrix to the total moment may not be applicable everyplace, but the constants seem reasonable when compared with the result in equation (A9). Therefore, we use

$$\dot{M}_{22} = -0.75\, \dot{M}_0. \tag{A10}$$

In an extensional environment, with $s > 0$, the numerical constant will also be positive. Combined with (A4), (A10) therefore gives

$$\dot{M}_0 = |2\mu l_1 l_3 s/0.75|. \tag{A11}$$

Substituting $s = \dot{\epsilon}_{22} l_2$ back into equation (A11) allows an estimate of seismic moments from geodetic strain.

## References


Allen, C. R. (1968). The tectonic environments of seismically active and inactive areas along the San Andreas fault system, in *Proceedings of the Conference on Geologic Problems of San Andreas Fault System,* W. R. Dickinson, and A. Grantz, Editors, Vol. XI, Stanford University Publications, Geological Sciences, Stanford, California.

Allen, C. R. (1975). Geological criteria for evaluating seismicity, *Bull. Geol. Soc. Am.* **86,** 1041–1057.

Allen, C. R., P. St. Amand, C. F. Richter, and J. M. Nordquist (1965). Relationship between seismicity and geologic structure in the southern California region, *Bull. Seism. Soc. Am.* **55,** 753–797.

Anderson, J. G. and M. D. Trifunac (1978). On uniform risk functionals which describe strong ground motion, *Bull. Seism. Soc. Am.* **68,** 205–214.

Atwater, T. (1970). Implications of plate tectonics for the Cenozoic tectonic evolution of western North America, *Bull. Geol. Soc. Am.* **81,** 3513–3536.

Atwater, T. and P. Molnar (1973). Relative motion of the Pacific and North American plates deduced from sea floor spreading in the Atlantic, Indian and South Pacific Oceans, in *Proceedings of the Conference on Tectonic Problems of the San Andreas Fault System,* R. L. Kovach and A. Nur, Editors, Vol. XIII, Stanford University Publications, Geological Sciences, Stanford, California.

Barnhart, J. T. and J. E. Slosson (1973). The Northridge Hills and associated faults—a zone of high seismic probability?, in *Geology, Seismicity and Environmental Impact,* D. E. Moran, J. E. Slosson, R. O. Stone, and C. A. Yelverton, Editors, Special Publication, Association of Engineering Geologists, University Publishers, Los Angeles, California. pp. 253–256.

Bender, P. L. and E. C. Silverberg (1975). Present tectonic-plate motions from lunar ranging, *Tectonophysics* **29,** 1–7.

Bolt, B. A., J. Stifler, and R. Uhrhammer (1977), The Briones Hills earthquake swarm of January 8, 1977, Contra Costa County, California, *Bull. Seism. Soc. Am.* **67,** 1555–1564.

Brune, J. N. (1968). Seismic moment, seismicity, and rate of slip along major fault zones, *J. Geophys. Res.* **73,** 777–784.

Campbell, K. W. (1977). The use of seismotectonics in the Bayesian estimation of seismic risk, UCLA-ENG-7744, School of Engineering and Applied Science, University of California, Los Angeles.

Campbell, K. W. (1978). An estimate of earthquake recurrence times from seismotectonic data on a fault, in *Proceedings of the First Annual California Section Conference,* Association of Engineering Geologists, Los Angeles, pp. 95–101.

Carter, B. (1971). Quaternary displacement on the Garlock fault, California, *Trans. Am. Geophys. Union* **52,** 350.

Chen, W. P. and P. Molnar (1977). Seismic moments of major earthquakes and the average rate of slip in central Asia, *J. Geophys. Res.* **82,** 2945–2969.

Chinnery, M. A. and R. G. North (1975). The frequency of very large earthquakes, *Science* **190,** 1197–1198.

Christensen, M. N. (1966). Late Cenozoic crustal movements in the Sierra Nevada of California, *Bull. Geol. Soc. Am.* **77,** 163–182.

Coates, R. J., R. T. Clark, C. C. Counselman III, I. I. Shapiro, H. F. Hinteregger, A. E. Rogers, and A. R. Whitney (1975). Very long baseline interferometry for centimeter accuracy geodetic measurements, *Tectonophysics* **29,** 9–18.

Cornell, C. A. (1968). Engineering seismic risk analysis, *Bull. Seism. Soc. Am.* **58,** 1583–1606.

Crowell, J. C. (1973). Problems concerning the San Andreas fault system in southern California, in *Proceedings of the Conference on Tectonic Problems of the San Andreas Fault System,* R. L. Kovach and A. Nur, Editors, Vol. XIII, Stanford University Publication in Geological Sciences, Stanford, California, pp. 125–135.

Crowell, J. C. (1975). The San Andreas fault in southern California, in *San Andreas Fault in Southern California, Special Report 118,* J. C. Crowell, Editor, California Division of Mines and Geology, pp. 7–27.

Davies, G. F. and J. N. Brune (1971). Regional and global fault slip rates from seismicity, *Nature Phys. Sci.* **229,** 101–107.

Davis, G. A. and B. Burchfiel (1973). Garlock fault: an intracontinental transform structure, southern California, *Bull. Geol. Soc. Am.* **85,** 1931–1944.

Dibblee, T. W., Jr. (1966). Geology of the central Santa Ynez mountains, Santa Barbara County, California, *Calif. Div. Mines Geol. Bull.* **186,** 99 pp.

Dibblee, T. W., Jr. (1975). Late Quaternary uplift of the San Bernardino mountains on the San Andreas and related faults, in *San Andreas Fault in Southern California, Special Report 118,* J. C. Crowell, Editor, California Division of Mines and Geology, 127-146.

Dickinson, W. R., D. S. Cowan, and R. S. Schweikert (1972). A test of new global tectonics: discussion, *Am. Assoc. Petrol. Geol.* **56,** 375-384.

Ehlert, K. W. and P. L. Ehlig (1977). The "polka-dot" granite and the rate of displacement on the San Andreas fault in southern California (abstract), 73rd Annual Meeting, Cordilleran Section, Geological Society of America, Sacramento, pp. 415-416.

Ehlig, P. L. (1973). History, seismicity, and engineering geology of the San Gabriel fault, in *Geology, Seismicity and Environmental Impact,* D. E. Moran, J. E. Slosson, R. O. Stone, and C. A. Yelverton, Editors, Special publication, Association of Engineering Geologists, University Publishers, Los Angeles, pp. 247-251.

Garfunkle, Z. (1974). Model for the late Cenozoic tectonic history of the Mojave Desert, California, and for its relation to adjacent regions, *Bull. Geol. Soc. Am.* **85,** 1931-1944.

Graham, S. A. and W. R. Dickinson (1978). Evidence for 115 kilometers of right slip on the San Gregorio-Hosgri fault trend, *Science* **119,** 179-181.

Hanks, T. C., J. A. Hileman, and W. Thatcher (1975). Seismic moments of the larger earthquakes of the southern California region, *Bull. Geol. Soc. Am.* **86,** 1131-1139.

Hart, E. W. (1976). Basic geology of the Santa Margarita area, San Luis Obispo County, California, *Calif. Div. Mines Geol. Bull.* **199,** 45 pp.

Heirtzler, J. E., G. O. Dickson, E. M. Herron, W. C. Pitman III, and X. LePichon (1968). Marine magnetic anomalies, geomagnetic field reversals, and motions of the ocean floor and continents, *J. Geophys. Res.* **73,** 2119-2136.

Hileman, J. A., C. R. Allen, and J. M. Nordquist (1973). Seismicity of the southern California region 1 January 1932 to 31 December 1972, Seismological Laboratory, California Institute of Technology, Pasadena, California.

Jennings, C. W. (1975). Fault map of California, California Division of Mines and Geology, Sacramento, California.

Johnson, T. L., J. Madrid, and T. Koczynski (1976). A study of micro seismicity in northern Baja California, Mexico, *Bull. Seism. Soc. Am.* **66,** 1921-1929.

Kanamori, H. (1977a). The energy release in great earthquakes, *J. Geophys. Res.* **82,** 2981-2987.

Kanamori, H. (1977b). Seismic and aseismic slip along subduction zones and their tectonic implications, in *Islands Arcs, Deep Sea Trenches and Back Arc Basins, Maurice Ewing Series 1,* M. Talwani, and W. C. Pitmann III, Editors, Am. Geophys. Union, Washington, D.C., pp. 163-174.

Kennedy, M. P. (1975). Geology of the San Diego metropolitan area, California, *Calif. Div. Mines Geol. Bull.* **200,** 1-39.

Kosloff, D. (1977). Numerical simulations of tectonic processes in southern California, *Geophys. J.* **51,** 487-501.

Kostrov, V. V. (1974). Seismic moment and energy of earthquakes, and seismic flow of rocks, *Izv. Acad. Sci. SSR, Phys. Solid Earth.* **1,** 23-40.

Lamar, D. L., P. M. Merifield, and R. J. Proctor (1974). Earthquake recurrence intervals on major faults in southern California, in *Geology, Seismicity and Environmental Impact,* D. E. Moran, J. E. Slosson, R. O. Stone, and C. A. Yelverton, Editors, Special publication, Association of Engineering Geologists, University Publishers, Los Angeles, pp. 265-275.

Lawrence, R. D. (1976). Strike slip faulting terminates the Basin and Range Province in Oregon, *Bull. Geol. Soc. Am.* **87,** 846-850.

Meyers, H. and C. A. vonHake (1976). *Earthquake Data File Summary,* National Geophysical and Solar-Terrestrial Data Center, Boulder, Colorado.

Michael, E. D. (1966). Large lateral displacement on Garlock fault, California, as measured from offset fault system, *Bull. Geol. Soc. Am.* **77,** 111-114.

Minster, J. B., T. H. Jordan, P. Molnar, and E. Haines (1974). Numerical modeling of instantaneous plate tectonics, *Geophys. J.* **36,** 541-576.

Prescott, W. H., J. C. Savage, and W. T. Kinoshita (1978). Strain accumulation in the western United States between 1970 and 1977 (in press).

Quick, G. L. (1973). Preliminary microzonation for surface faulting in the Ventura, California, area, in *Geology, Seismicity and Environmental Impact,* D. E. Moran, J. E. Slosson, R. O. Stone, and C. A. Yelverton, Editors, Special publication, Association of Engineering Geologists, University Publishers, Los Angeles, pp. 257-264.

Richter, C. F. (1958). Elementary seismology, W. H. Freeman and Co., San Francisco, 768 pp.

Ryall, A. (1977). Earthquake hazard in the Nevada region, *Bull. Seism. Soc. Am.* **58,** 1583-1606.

Sage, O., Jr. (1973). Paleocene geography of the Los Angeles region, in *Proceedings of the Conference on Tectonic Problems of the San Andreas Fault System,* R. L. Kovach, and A. Nur, Editors, Stanford University Publications, Geological Sciences, Vol. XIII, Stanford, California, pp. 348-357.

Savage, J. C. and R. O. Burford (1970). Accumulation of tectonic strain in California, *Bull. Seism. Soc. Am.* **60,** 1877-1896.

Savage, J. C. and R. O. Burford (1973). Geodetic determination of relative plate motion in central California, *J. Geophys. Res.* **78,** 832–845.

Savage, J. C., J. P. Church, and W. H. Prescott (1975). Geodetic measurement of deformation in Owens Valley, California, *Bull. Seism. Soc. Am.* **66,** 865–874.

Savage, J. C. and W. H. Prescott (1976). Strain accumulation on the San Jacinto fault near Riverside, California, *Bull. Seism. Soc. Am.* **66,** 1749–1754.

Scholz, C. H., L. R. Sykes, and Y. Aggarwal (1973). Earthquake prediction: a physical basis, *Science* **181,** 803–810.

Sharp, R. V. (1967). San Jacinto fault zone in the penisular ranges of southern California, *Bull. Geol. Soc. Am.* **78,** 705–730.

Sieh, K. E. (1977). A study of Holocene displacement history along the south-central reach of the San Andreas fault, *Ph.D. Thesis,* Stanford University, Stanford, California, 219 pp.

Slemmons, D. B. (1977). State-of-the-art for assessing earthquake hazards in the United States, Report 6, faults and earthquake magnitude, Miscellaneous paper S-73-1, U.S. Army Engineer Waterways Experiment Station, Soils and Pavements Laboratory, Vicksburg, Miss., 167 pp.

Shepard, F. P. and K. O. Emery (1941). Submarine topography off the California coast: canyons and tectonic interpretation, *Geol. Soc. Am.,* Spec. Paper 31, 171 pp.

Smith, G. I. (1962). Large lateral displacement on Garlock fault, California, as measured from offset dike swarms, *Am. Assoc. Petrol. Geol. Bull.* **46,** 85–104.

Smith, R. S. U. (1977). Late Quaternary seismicity and rates of tectonic deformation, Panamint Valley, California (abstract), in *Summaries of Technical Reports, Vol. IV,* submitted to National Earthquake Hazards Reduction Program, J. D. Everenden, Editor, Office of Earthquake Studies, Menlo Park, California, p. 133.

Smith, S. W. (1976). Determination of maximum earthquake magnitude, *Geophys. Res. Letters* **3:** 351–354.

Stepp, J. C. (1972). Analysis of completeness of the earthquake sample in the Puget Sound area and its effect on statistical estimates of earthquake hazard, *Proc. Intern. Conf. Microzonation for Safer Const., Res., Appl.,* Seattle, Washington Univ. **2,** 897–909.

Thatcher, W. and T. C. Hanks (1973). Source parameters of southern California earthquakes, *J. Geophys. Res.* **78,** 8547–8576.

Thatcher, W., J. A. Hileman, and T. C. Hanks (1975). Seismic slip distribution along the San Jacinto fault zone, southern California, and its implications, *Bull. Geol. Soc. Am.* **86,** 1140–1146.

Walcott, R. I. (1978). Present tectonics and late Cenozoic evolution of New Zealand, *Geophys. J.* **52,** 137–164.

Wallace, R. E. (1976). Seismicity of north-central Nevada on the basis of young fault scarps (abstract), *Earthquake Notes* **47,** 21–22.

Weber, F. H., Jr. (1977). Total right lateral offset along the Elsinore fault zone, southern California (abstract), 73rd Annual Meeting, Cordilleran Section, Geological Society of America, Sacramento, 524.

Weber, G. E. and K. R. Lajoie (1977). Late Pleistocene and Holocene tectonics of the San Gregorio fault zone between Moss Beach and Point Ano Nuevo, San Mateo County, California (abstract), 73rd Annual Meeting, Cordilleran Section, Geological Society of America, Sacramento, 524.

Wright, L. A. and B. W. Troxel (1967). Limitations on right-lateral, strike-slip displacements, Death Valley and Furnace Creek fault zones, California, *Bull. Geol. Soc. Am.* **78,** 933–950.

Wright, T. L., E. S. Parker, and R. C. Erickson (1973). Stratigraphic evidence for timing and nature of late Cenozoic deformation in Los Angeles region, California (abstract), *Am. Assoc. Petrol. Geol. Bull.* **57,** 813.

Yeates, R. S. (1973). Newport-Inglewood fault zone, Los Angeles Basin, California, *Am. Assoc. Petrol. Geol. Bull.* **57,** 117–135.

Yerkes, R. F., T. H. McCulloch, J. E. Schoellhamer, and J. G. Vedder (1965). Geology of the Los Angeles Basin, California—an introduction, *U.S. Geol. Survey Profess. Paper 420-A,* Washington, D.C., 57 pp.

School of Engineering
Department of Civil Engineering
University of Southern California
Los Angeles, California 90007

Manuscript received May 19, 1978